Hydrogen adsorption on phosphorus-rich (2×1) indium phosphide (001)

Q. Fu,[1] E. Negro,[2] G. Chen,[1] D. C. Law,[1] C. H. Li,[1] R. F. Hicks,[1,*] and Krishnan Raghavachari[3]
[1]*Department of Chemical Engineering, University of California, Los Angeles, California 90095*
[2]*Department of Physics, University of Padova, Italy 35131*
[3]*Materials Research, Agere Systems, Murray Hill, New Jersey 07974*
(Received 9 May 2001; revised manuscript received 25 September 2001; published 1 February 2002)

Hydrogen adsorption on the InP (001)-(2×1) reconstruction has been characterized by vibrational spectroscopy and *ab initio* calculations with density functional theory. The (2×1) surface is covered with a complete layer of phosphorus dimers. The clean and hydrogen-terminated dimers have been modeled by $In_5P_4H_x$ clusters with the proper number of covalent and dative bonds to accurately represent the surface of interest. The optimized molecular cluster of the unreacted dimer reveals that it has one filled and one partially filled dangling bond. Hydrogen atoms attack the P-P dimers forming terminal and coupled phosphorus-hydrogen bonds, and the predicted vibrational frequencies of these species are in excellent agreement with the infrared spectra. All the observed vibrational modes can be assigned to species containing one, two, and three hydrogen bonds (i.e., PH, HP-PH, and $PH+PH_2$) per surface dimer.

DOI: 10.1103/PhysRevB.65.075318 PACS number(s): 31.15.Ar, 78.55.Cr, 68.35.Bs, 78.30.−j

I. INTRODUCTION

Compound semiconductors are an interesting class of materials that are widely employed by the electronics industry.[1–5] An important application of these materials is in optoelectronic devices, owing to their direct band gap and high carrier mobility that set them apart from silicon.[6] It is well known that the performance of a compound semiconductor device strongly depends upon the vapor-phase growth process.[7,8] In particular, the structure and composition of the surface during epitaxy translate directly into the structure and composition of the bulk film. Therefore, a thorough understanding of the surface physics of compound semiconductors can help in further optimizing the processes used to fabricate devices.

The (001) plane of III-V compound semiconductors may be terminated with either group-III or group-V atoms, depending on the preparation method. In the ideal case, each exposed atom has two dangling bonds. However, to minimize the total surface energy, one of the dangling bonds is eliminated by forming dimers between neighboring atoms, which gives rise to long-range ordering on the surface.[9–14] Scanning tunneling microscopy (STM) is one of the principal methods used to investigate the surface structure of semiconductors. Nevertheless, difficulties can arise in interpreting STM images, because geometric and electronic effects are folded together in the voltage trace measured by the instrument.[15] To overcome this drawback, it is important to complement this technique with other surface probes, such as infrared spectroscopy of adsorbed hydrogen.[11,16–21] Definitive assignments of the *M-H* vibrational modes is accomplished by building cluster models of the adsorption sites and then optimizing the cluster structure using *ab initio* calculations with density functional theory (DFT).[19–27]

Over the past several years, we have been studying the atomic structure of indium phosphide (001) surfaces produced by metalorganic vapor-phase epitaxy (MOVPE).[11,28–30] The most stable phosphorus-rich reconstruction is (2×1), which consists of a single monolayer of phosphorus dimers.[11] The phosphorus termination was confirmed by the infrared spectrum of adsorbed hydrogen, which contained a series of bands between 2350 and 2200 cm^{-1} due to P-H stretching vibrations, and not In-H stretching vibrations. The large number of bands observed indicates that hydrogen forms a variety of different chemical bonds to the exposed P atoms.

In this paper, we analyze the structure and vibrational properties of the clean and hydrogen-terminated phosphorus dimers with the aid of molecular cluster calculations. The unreacted dimer exhibits an electronic structure with the presence of one half-filled and one filled dangling orbital. Hydrogen atoms attack the dangling bonds as well as the phosphorus dimer bonds, generating several PH and PH_2 adsorbate structures. The predicted vibrational modes of these species are in excellent agreement with the experimental results.

II. EXPERIMENTAL METHODS

Indium phosphide films, 0.5 μm thick, were grown on InP (001) substrates by organometallic vapor-phase epitaxy.[11] The following conditions were used during growth: 600 °C, 20 Torr of hydrogen, 6.5×10^{-4} Torr of tri-isopropyl indium (TIPIn), 0.13 Torr of tertiarybutylphosphine (TBP) (V/III ratio of 200), and a total flow rate of 2.5 1/min at 25 °C and 760 Torr. After shutting off the TIPIn supply, the TBP and hydrogen flows were maintained until the samples were cooled to 300 and 40 °C, respectively. Then the crystals were transferred directly to an ultrahigh-vacuum chamber without air exposure. In vacuum, the samples were annealed in 1×10^{-5} Torr of phosphine for 30 min at 300 °C to obtain the (2×1) reconstruction. After cooling the samples to 25 °C, the surface structure was characterized by low-energy electron diffraction (LEED) and STM.[11] The images obtained with the latter analytical technique were of the filled states at a bias of −3.0 V and with a tunneling current of 0.5 nA.

The infrared spectra were recorded by multiple internal reflections through a trapezoidal InP crystal, $40.0\times10.0\times0.64$ mm^3. This crystal provided for 31 reflections off the

front face. Two substrate orientations were examined: one with the long crystal axis parallel to the $[\bar{1}10]$ direction and one with the long crystal axis parallel to the [110] direction. Hydrogen was introduced into the chamber at 5×10^{-7} Torr and dissociated to atoms by a tungsten filament located 4 cm from the sample face. The flux of H atoms relative to H_2 molecules was estimated to be 0.1%.[18] The surface was saturated following a continuous hydrogen dosing for 30 min (900 L H_2 or ~1 L of H, 1 $L=10^{-6}$ Torr·S). A series of vibrational spectra was collected before and during hydrogen adsorption with a BIORAD FTS-40 A spectrometer. These spectra were recorded at 8 cm^{-1} resolution and by co-adding 1024 scans. The spectra presented in this paper show the change in reflectance (per reflection) that results from taking the ratio of the sample spectrum with adsorbed hydrogen to that of the clean surface. In addition to the infrared measurements, LEED patterns were recorded during hydrogen dosing.

III. THEORETICAL METHODS

The quantum chemistry calculations were performed on molecular clusters having one phosphorus dimer in its immediate bonding environment. In particular, the clusters contained a single phosphorus dimer tethered to five ''bulk'' In atoms and two ''bulk'' P atoms. This is analogous to the cluster containing nine silicon atoms that has been used to represent a single dimer on the Si (100) surface.[22] Typically, the truncated bulk bonds in the clusters are terminated with hydrogen atoms to eliminate artifacts due to excess spin or charge. However, the situation is more complicated with indium phosphide due to the presence of both covalent and dative contributions to the bonding. The four bonds around each In or P atom can be considered as composed of three covalent bonds and one dative bond. While a truncated covalent bond can be terminated with hydrogen, a different procedure is needed to terminate the dative bonds.

In previous work on GaAs (001) surfaces, the dative bonds were ignored by making some of the gallium atoms threefold coordinated.[19] However, this is unsatisfactory and leads to unphysical bridging hydrides in bulk atom positions. In this work, the truncated dative bonds at bulk indium atoms are replaced by dative bonds to PH_3 groups. Two datively bonded groups per cluster result in a physically realistic model, where charge neutrality is achieved while maintaining each atom in fourfold coordination. More details about this procedure will be discussed in a future publication. Hydrogen atoms are then added to the surface phosphorus atoms resulting in different PH and PH_2 species.

The GAUSSIAN98 quantum chemistry suite was used to optimize the structure of each $In_5P_4H_x$ cluster and predict its vibrational properties.[31] These calculations were made utilizing density functional theory with the Becke three-parameter exchange functional and the Lee-Yang-Parr correlation functional (B3LYP).[32,33] We chose the $(18s/14p/9d)/[6s/5p/3d]$ contracted basis set for indium, the Dunning-Huzinaga $(11s/7p/1d)/[6s/4p/1d]$ contracted basis set (D95**) for phosphorus, the D95** polarized double-ζ basis set for the surface hydrogen atoms, and the D95 double-ζ basis set for the terminating hydrogens.[34,35] No geometric constraints were placed on the optimization process, and no negative vibrational frequencies were observed for the final structures. It should be noted that the predicted values have been shifted down by 110 cm^{-1} to correct for systematic errors, such as the neglect of anharmonicity, deficiencies in the density functionals, etc. This provides a self-consistent method of comparing the vibrational modes exhibited by each type of bond. Weldon *et al.* have used this same approach with a similar shift to characterize the hydrogen bonds formed on silicon surfaces.[36]

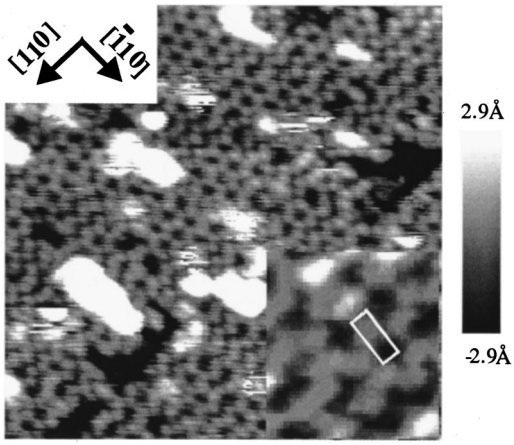

FIG. 1. Filled-states scanning tunneling micrograph of the (2×1) reconstruction (Ref. 6). The image area is 190×190 Å^2. The contrast from black to white corresponds to a height change of 5.8 Å^2.

IV. RESULTS AND DISCUSSION

To interpret the vibrational spectra, we must now consider the atomic structure of the (2×1) reconstruction. A filled-states scanning tunneling micrograph of the P-rich (2×1) surface is shown in Fig. 1.[11] A series of zigzagging rows of gray spots is seen extending along the [110] crystal direction. The white and black patches interspersed throughout the picture are due to small areas located two atomic layers above and below the primary surface plane. Decreasing the contrast reveals that these patches have the same (2×1) structure.

A ball-and-stick model of the (2×1) reconstruction is presented in Fig. 2. The surface is terminated with a complete monolayer of phosphorus dimers.[11] The valence elec-

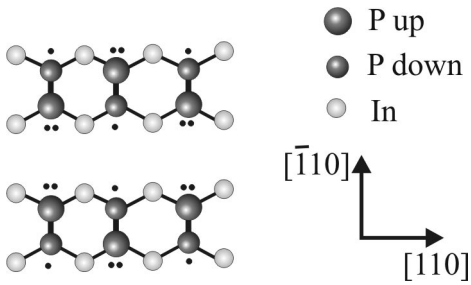

FIG. 2. Ball-and-stick model of the (2×1) reconstruction. The small dots represent the valence electrons in the dangling orbitals.

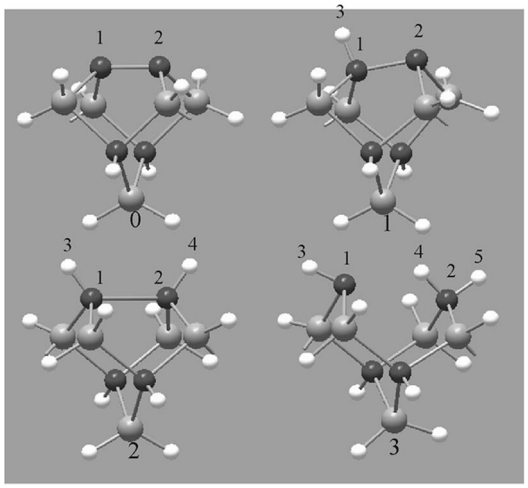

FIG. 3. Models of the optimized molecular clusters, illustrating the different ways hydrogen atoms coordinate to a phosphorus dimer. The P, In, and H atoms are black, gray, and white spheres, respectively. The open valences at the second layer In atoms denote dative bonding to PH_3 groups (see text).

tron distribution of the (2×1) can be understood as follows. In the unit cell, there are two top-layer P atoms and two second-layer In atoms. The second-layer atoms contribute half their valence electrons (3) to the bonding, while the top-layer atoms contribute all their valence electrons (10) to the bonding. Out of the 13 total electrons, the 4 In-P backbonds and the surface dimer bond consume 10 electrons. Thus three valence electrons are distributed between the two dangling bonds on each dimer. These are indicated by the black dots in the model.

An optimized molecular cluster of the dimer, $In_5P_4H_{10}$ (with two dative PH_3 groups), is shown as structure **0** in Fig. 3. Interestingly, this structure has two equivalent P atoms (no buckling) with the unpaired electron being shared by the two surface atoms. However, asymmetric environments around the two surface atoms do lead to buckling. For example, a slightly different isomer where one of the two dative PH_3 groups is attached to a fourth-layer In atom shows buckling. In addition, attachment of a single hydrogen atom to the surface dimer leads to buckling (cluster **1** in Fig. 3). In such cases, the phosphorus atom containing the lone pair of electrons is pushed up and out of the surface plane, while the phosphorus atom containing the single electron is pulled down. This is consistent with the STM image in Fig. 1, showing buckled dimers alternating to the left and right as one proceeds along the row in the [110] direction. Presumably, the alternating direction of the buckling along the row relieves some of the strain on the In-P backbonds. Larger cluster calculations containing multiple dimer units may be necessary to fully resolve the electronic structure associated with the phosphorus dimer.

In our previous paper on the (2×1), we measured a surface bandgap of 1.2 ± 0.2 eV by scanning tunneling spectroscopy.[11] This was explained by electron correlation between the singly occupied states. A more accurate description of this surface may be that of a Mott insulator, due to the large separation between the unpaired electrons, $\sim$6 Å.[37,38] A

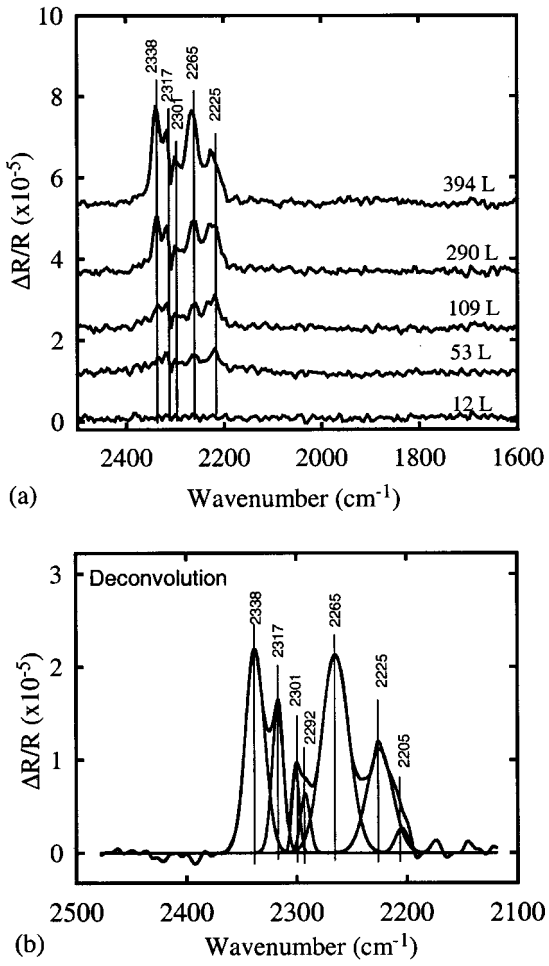

FIG. 4. Infrared reflectance spectra of adsorbed hydrogen on (2×1) InP (001) at 25 °C: (a) as a function of H_2 dosage and (b) at full coverage showing the deconvolution of the bands.

semiconducting local density of states is observed because the Coulomb repulsion experienced by the electrons creates a Hubbard gap (in the range of 1.0 eV). It is interesting to note that our small cluster containing a single surface dimer has a low-lying electronic excitation from the filled to the partially filled dangling orbital at 1.4 eV (with time-dependent B3LYP density functional theory).[39]

Hydrogen atoms were dosed onto the InP (001) (2×1) surface in the UHV chamber at 5×10^{-7} Torr. As the hydrogen dosing proceeds, the (2×1) LEED pattern gradually converts to (1×1), indicating that the hydrogen atoms react with the phosphorus dimers, breaking some of the P-P bonds and disrupting the surface ordering. Shown in Fig. 4 are a series of infrared reflectance spectra for different hydrogen coverages on the (2×1) at 298 K. Also shown in the figure is the deconvoluted infrared spectrum corresponding to saturation coverage. Five overlapping but clearly resolved peaks are observed at 2338, 2317, 2301, 2265, and 2225 cm^{-1}. In addition, weak shoulders may be present at 2292 and 2205 cm^{-1}. No features are seen in the region between 1700 and 1200 cm^{-1}, where indium hydride stretching vibrations occur.[11] The assignment of each band to a specific adsorbate

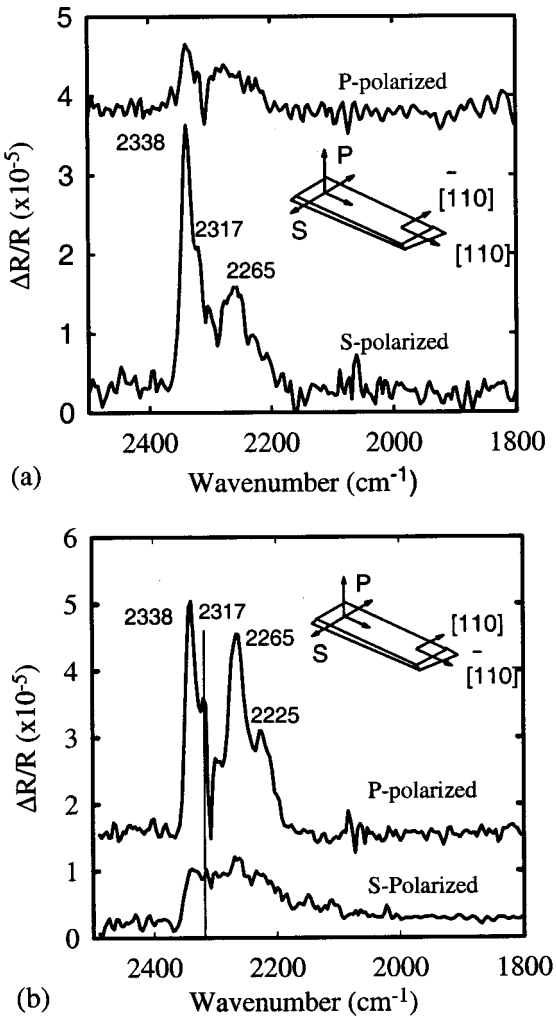

FIG. 5. Polarized infrared reflectance spectra of hydrogen adsorbed on the (2×1) surface, with the long crystal axis parallel to (a) the [110] direction and (b) the $[\bar{1}10]$ direction.

structure can be made by comparison to the cluster models, as discussed below.

Presented in Fig. 5 are polarized infrared reflectance spectra of hydrogen adsorbed at saturation coverage on the (2×1) surface for two orientations of the indium phosphide crystal. The inset diagrams in the figures show the direction of the polarization relative to the crystal directions. The P-H vibrational bands are more strongly *p* polarized when the long axis of the crystal is parallel to the $[\bar{1}10]$, whereas they are more strongly *s* polarized when the long axis of the crystal is parallel to the [110]. This optical anisotropy is consistent with a situation where most of the P-H bonds are oriented primarily in a plane swept out by the [001] and $[\bar{1}10]$ axis. Although poorly defined, the intensities of the *s*-polarized spectrum in Fig. 4(b) are not zero. This means that the transition dipole moments of the P-H bonds have some residual value in the [110] direction.

Figure 3 shows a sequence of molecular clusters (Nos. **1**, **2**, and **3**) that represent the addition of one, two, and three hydrogen atoms to a phosphorus dimer on the indium phosphide (001) (2×1) surface. Note that atoms numbered 1 and 2 in clusters **1–3** represent the phosphorus dimer atoms on the surface, while the other atoms constitute the ''bulk crystal'' to which the dimer is tethered. Although not shown in the models, the dangling bonds on atom 2 in cluster **1** and atom 1 in cluster **3** are each filled with a lone pair of electrons. Examination of the figure reveals that one H atom can be added to the dimer to yield a single P-H bond. As mentioned earlier, this asymmetry in the surface environment causes this dimer to buckle. The addition of a second hydrogen leads to a symmetric structure with a coupled H-P-P-H species and an elongated P-P bond. Finally, the addition of a third hydrogen atom breaks the dimer bond, yielding a saturated cluster with a PH and a PH_2 group.

The P-H vibrational modes calculated for clusters **1–3** are listed in Table I. Also shown in the table are the frequencies and intensities of the infrared bands observed for hydrogen adsorption on the (2×1) reconstruction. Excellent agreement is achieved between the theory and the experiments. The P-H bond in (**1**) exhibits a single mode with medium intensity at 2301 cm^{-1}. This mode requires no P-P bond breakage and is assigned to the experimentally observed peak at 2302 cm^{-1}. The coupled monohydrogen structure (**2**) exhibits asymmetric and symmetric stretching vibrations at 2256 and 2260 cm^{-1}. The asymmetric stretch is of weaker intensity and produces a dipole moment parallel to the phosphorus dimer bond (i.e., the $[\bar{1}10]$ crystal axis). On the other

TABLE I. Vibrational modes observed for the hydrogen-terminated (2×1) surfaces. as=asymmetric, s=symmetric.

	Theory			Experiment	
Assignment	Frequency (cm^{-1})	Intensity	Cluster[a]	Frequency (cm^{-1})	Intensity
P_1-H_3	2302	m	**1**	2301	m
H_3-P_1P_2-H_4^{as}	2256	m	**2**	2265	s
H_3-P_1P_2-H_4^{s}	2260	s	**2**	2265	s
:P_1-H_3	2238	s	**3**	2225	s
H_4-P_2-H_5^{s}	2315	m	**3**	2317	m
H_4-P_2-H_5^{as}	2333	m	**3**	2338	s

[a]Refer to Fig. 5.

TABLE II. Bond lengths and bond angles for the phosphorus-rich clusters (bond length in Å).

Parameters	Cluster No.		
	1	**2**	**3**
$P_1 \cdots P_2$	2.259	2.977	4.056
P_1-H_3	1.418	1.425	1.429
P_2-H_4		1.425	1.417
P_2-H_5			1.418
$\angle H_3$-$P_1 \cdots P_2$	102.6°	124.9°	160.7
$\angle H_4$-P_2-H_5			99.5

hand, the symmetric stretch is strong in intensity and has a dipole moment perpendicular to the surface plane. This mode corresponds closely to the broad band recorded at 2265 cm^{-1} on the H-(2×1) surface. Measurements made with polarized light agree for the most part with the predicted dipole moments. For example, if the infrared beam travels parallel to the $[\bar{1}10]$ axis, the 2265 cm^{-1} band is very intense with *p* polarization.

The saturated cluster containing the PH and PH_2 groups (**3**) has a strong monohydrogen mode at 2238 cm^{-1} and explains the experimental band at 2225 cm^{-1}. Its low frequency is due to the presence of the lone pair and is consistent with its slightly longer P-H bond length, as seen in Table II. The di-hydrogen modes are split by about 18 cm^{-1} with the asymmetric stretch being higher in frequency. The predicted positions 2315 and 2333 cm^{-1} are in excellent agreement with the experimental infrared peaks seen at 2317 and 2338 cm^{-1}. The fact that the modes from **2** and **3** are seen at higher hydrogen exposure is consistent with their requiring P-P bond breakage.

Dielectric screening by the semiconductor surface reduces the intensity of vibrations normal to the crystal plane.[19,21,39] We estimate that this should decrease by about fourfold the intensity of the modes perpendicular to the surface, which are the symmetric vibrations of the coupled H-P-P-H and PH_2 species. This may explain the weak intensity of the mode at 2317 cm^{-1}. After accounting for the impact of dielectric screening, the band intensities predicted by the theory are in good qualitative agreement with the experiments.

Listed in Table II are some of the bond lengths and bond angles obtained for the optimized clusters **1–3**. On cluster **0**, before hydrogen adsorption, we calculate a phosphorus dimer bond length of 2.165 Å. Adsorption of hydrogen onto the terminal site of the phosphorus dimer, as in **1**, causes the P-P bond to lengthen to 2.259 Å. The P_1-H_3 bond length for the fourfold-coordinated P atom in **1** is 1.418 Å. This may be compared to the phosphorus-hydrogen bond on cluster **3**, where a lone pair of electrons remains in the dangling bond. In the latter case, the P_1-H_3 bond length is 1.429 Å. The shortening of the P-H bond on the fourfold-coordinated atoms is primarily due to the mixing of *s* and *p* atomic orbitals, which eliminates electron screening. Conversely, the lone pair of electrons on the threefold-coordinated P atoms populates the unmixed $3s$ orbital and effectively screens the nucleus from the H atom. In cluster **3**, the $\angle H_3$-P_1-P_2 bond angle of 161° puts the P-H bond at nearly a right angle to the In-P backbonds, as expected for the use of predominately $3p$ orbitals in bond formation. Our results agree with the study of the H_3Al-PH_3 adduct by Davy and Schaefer.[40] These authors demonstrated that removing the lone pair of electrons on phosphine by dative bonding with AlH_3 shortens the P-H bond length by 0.012 Å.

It is interesting that for PH_2, the asymmetric stretch is predicted at a frequency 18 cm^{-1} higher than the symmetric stretch. By contrast, the asymmetric stretch of the coupled H-P-P-H group is predicted to occur 4 cm^{-1} lower than the symmetric stretch. A similar reversal has been seen previously for SiH_2 (asymmetric stretch higher) and H-Si-Si-H (symmetric stretch higher).

V. CONCLUSIONS

We have characterized the adsorption of hydrogen on the InP (001)-(2×1) surface by vibrational spectroscopy and *ab initio* cluster calculations with density functional theory. The series of infrared bands observed for H:(2×1) can be explained by an attack of hydrogen atoms at the dangling bond and dimer bond sites, generating both PH and PH_2 bonds. Moreover, the quantum chemistry calculations predict that the unreacted phosphorus dimer exhibits partially filled and filled dangling orbitals, which is consistent with the STM results. We have found that to accurately simulate the dimer chemistry on III/V compound semiconductor surfaces using DFT, one must account for the covalent and dative bonding among the group-III and V atoms.

ACKNOWLEDGMENTS

The authors are grateful for the funding provided by the National Science Foundation, Division of Materials Research and Chemical and Transport Systems. We thank M. L. Steigerwald for some stimulating discussions.

*Corresponding author. Electronic address: rhicks@ucla.edu

[1] K. A. Jackson, *Compound Semiconductor Devices: Structures and Processing* (Wiley-VCH, Weinheim, Germany, 1998).
[2] Compound Semiconductor 1–7 (1995–2001).
[3] Y. Matsuoka, K. Kurishima, and T. Makimoto, IEEE Electron Device Lett. **EDL-14**, 357 (1993).
[4] M. Sugo, H. Mori, Y. Sakai, and Y. Itoh, Appl. Phys. Lett. **60**, 472 (1992).
[5] K. Mobarhan, C. Jelen, E. Kolev, and M. Razeghi, J. Appl. Phys. **74**, 743 (1993).
[6] V. Swaminathan and A. T. Macrander, *Materials Aspects of GaAs and InP Based Structures* (Prentice Hall, Englewood Cliffs, NJ, 1991).
[7] G. B. Stringfellow, *Organometallic Vapor-Phase Epitaxy: Theory and Practice* (Academic, San Diego, 1989).
[8] Q. Fu, L. Li, M. J. Begarney, B.-K. Han, D. C. Law, and R. F.

Hicks, J. Phys. IV **9**, Pr8-3 (1999).
[9] M. D. Pashley, Phys. Rev. B **40**, 10 481 (1989).
[10] D. J. Chadi, J. Vac. Sci. Technol. A **5**, 834 (1987).
[11] L. Li, B.-K. Han, Q. Fu, and R. F. Hicks, Phys. Rev. Lett. **82**, 1879 (1999).
[12] J. E. Northrup and S. Froyen, Phys. Rev. B **50**, 2015 (1994).
[13] Q. K. Xue, T. Hashizume, and T. Sakurai, Prog. Surf. Sci. **56**, 1 (1997).
[14] L. Li, B.-K. Han, S. Gan, H. Qi, and R. F. Hicks, Surf. Sci. **398**, 386 (1998).
[15] J. Tersoff and N. D. Lang, *Scanning Tunneling Microscopy* (Academic, San Diego, 1993).
[16] H. Qi, P. E. Gee, and R. F. Hicks, Phys. Rev. Lett. **72**, 250 (1994).
[17] H. Qi, P. E. Gee, T. Nguyen, and R. F. Hicks, Surf. Sci. **323**, 6 (1995).
[18] R. F. Hicks, H. Qi, Q. Fu, B.-K. Han, and L. Li, J. Chem. Phys. **110**, 10498 (1999).
[19] Q. Fu, L. Li, and R. F. Hicks, Phys. Rev. B **61**, 11 034 (2000).
[20] Y. J. Chabal and K. Raghavachari, Phys. Rev. Lett. **53**, 282 (1984).
[21] Y. J. Chabal, Surf. Sci. Rep. **8**, 211 (1988).
[22] B. B. Stefanov and K. Raghavachari, Surf. Sci. **389**, L1159 (1997).
[23] J. Eng, K. Raghavachari, L. M. Struck, Y. J. Chabal, B. E. Bent, M. M. Banaszak-Holl, F. R. McFeely, A. M. Michaels, G. W. Flynn, S. B. Christman, E. E. Chaban, G. P. Williams, K. Radermacher, and S. Mantl, J. Chem. Phys. **108**, 8680 (1998).
[24] J. Shan, Y. Wang, and R. J. Hamers, J. Phys. Chem. **100**, 4961 (1996).
[25] Y. Miyamoto and S. Nonoyama, Phys. Rev. B **46**, 6915 (1992).
[26] G. Brocks, P. J. Kelly, and R. Car, Phys. Rev. Lett. **66**, 1729 (1991).
[27] L. G. LePage, M. Alouani, D. L. Dorsey, J. W. Wilkins, and P. E. Blochl, Phys. Rev. B **58**, 1499 (1998).
[28] L. Li, B.-K. Han, D. Law, C. H. Li, Q. Fu, and R. F. Hicks, Appl. Phys. Lett. **75**, 683 (1999).
[29] L. Li, Q. Fu, C. H. Li, B.-K. Han, and R. F. Hicks, Phys. Rev. B **61**, 10 223 (2000).
[30] M. J. Begarney, C. H. Li, D. C. Law, S. B. Visbeck, Y. Sun, and R. F. Hicks, Appl. Phys. Lett. **78**, 55 (2001).
[31] M. J. Frisch, G. W. Trucks, H. B. Schlegel, G. E. Scuseria, M. A. Robb, J. R. Cheeseman, V. G. Zakrzewski, J. A. Montgomery, R. E. Stratmann, J. C. Burant, S. Dapprich, J. M. Millam, A. D. Daniels, K. N. Kudin, M. C. Strain, O. Farkas, J. Tomasi, V. Barone, M. Cossi, R. Cammi, B. Mennucci, C. Pomelli, C. Adamo, S. Clifford, J. Ochterski, G. A. Petersson, P. Y. Ayala, Q. Cui, K. Morokuma, D. K. Malick, A. D. Rabuck, K. Raghavachari, J. B. Foresman, J. Cioslowski, J. V. Ortiz, B. B. Stefanov, G. Liu, A. Liashenko, P. Piskorz, I. Komaromi, R. Gomperts, R. L. Martin, D. J. Fox, T. Keith, M. A. Al-Laham, C. Y. Peng, A. Nanayakkara, C. Gonzalez, M. Challacombe, P. M. W. Gill, B. G. Johnson, W. Chen, M. W. Wong, J. L. Andres, M. Head-Gordon, E. S. Replogle, and J. A. Pople, *Gaussian 98 (Rev. A.7*) (Gaussian, Inc., Pittsburgh, PA, 1998).
[32] A. D. Becke, J. Phys. Chem. **98**, 1372 (1993).
[33] C. T. Lee, W. T. Yang, and R. G. Parr, Phys. Rev. B **37**, 785 (1988).
[34] N. Godbout, D. R. Salahub, J. Andzelm, and E. Wimmer, Can. J. Chem. **70**, 560 (1992).
[35] T. H. Dunning, P. J. Hay, and H. F. Schaefer III, *Modern Theoretical Chemistry* (Plenum, New York, 1976).
[36] M. K. Weldon, K. T. Queeney, A. B. Gurevich, B. B. Stefanov, Y. J. Chabal, and K. Raghavachari, J. Chem. Phys. **113**, 2440 (2000).
[37] N. F. Mott, Rev. Mod. Phys. **40**, 677 (1968).
[38] N. F. Mott, Proc. Phys. Soc. London, Sect. A **62**, 416 (1949).
[39] R. E. Stratmann, G. E. Scuseria, and M. J. Frisch, J. Chem. Phys. **109**, 8218 (1998).
[40] R. D. Davy and H. F. Schaefer III, J. Phys. Chem. A **101**, 3135 (1997).